Effects of the Loss of Conjunctival Muc16 on Corneal Epithelium and Stroma in Mice

Kumi Shirai,[1] Yuka Okada,[1] Dong-Joo Cheon,[2,3] Masayasu Miyajima,[4] Richard R. Behringer,[2,3] Osamu Yamanaka,[1] and Shizuya Saika[1]

[1]Department of Ophthalmology, Wakayama Medical University School of Medicine, Wakayama, Japan
[2]Program in Genes and Development, The University of Texas Graduate School of Biomedical Sciences at Houston, Houston, Texas, United States
[3]Department of Genetics, University of Texas MD Anderson Cancer Center, Houston, Texas, United States
[4]The Laboratory Animal Center, Wakayama Medical University School of Medicine, Wakayama, Japan

Correspondence: Kumi Shirai, Department of Ophthalmology, Wakayama Medical University School of Medicine, 811-1 Kimiidera, Wakayama, 641-0012, Japan; shirai@wakayama-med.ac.jp.

Submitted: July 31, 2013
Accepted: April 14, 2014

Citation: Shirai K, Okada Y, Cheon D-J, et al. Effects of the loss of conjunctival Muc16 on corneal epithelium and stroma in mice. *Invest Ophthalmol Vis Sci*. 2014;55:3626–3637. DOI:10.1167/iovs.13-12955

Purpose. To examine the role of conjunctival Muc16 in the homeostasis of the ocular surface epithelium and stroma using Muc16-null knockout (KO) mice.

Methods. We used KO mice (n = 58) and C57/BL6 (WT) mice (n = 58). Histology and immunohistochemistry were employed to analyze the phenotypes in the ocular surface epithelium. The expression of phospho-Stat3, AP-1 components, interleukin 6 (IL-6), and tumor necrosis factor-α (TNFα) in the cornea and conjunctiva was examined. The shape of the nuclei of corneal epithelial cells was examined to evaluate intraepithelial cell differentiation. Epithelial cell proliferation was studied using bromo-deoxyuridine labeling. Finally, the wound healing of a round defect (2-mm diameter) in the corneal epithelium was measured. The keratocyte phenotype and macrophage invasion in the stroma were evaluated after epithelial repair.

Results. The loss of Muc16 activated Stat3 signal, affected JunB signal, and upregulated the expression of IL-6 in the conjunctiva. Basal-like cells were observed in the suprabasal layer of the corneal epithelium with an increase in proliferation. The loss of Muc16 accelerated the wound healing of the corneal epithelium. The incidence of myofibroblast appearance and macrophage invasion were more marked in KO stroma than in WT stroma after epithelial repair.

Conclusions. The loss of Muc16 in the conjunctiva affected the homeostasis of the corneal epithelium and stroma. The mechanism might include the upregulation of the inflammatory signaling cascade (i.e., Stat3 signal, and IL-6 expression in the KO conjunctiva). Current data provides insight into the research of the pathophysiology of dry eye syndrome.

Keywords: membrane-associated mucin, Muc16, cytokine, cornea, conjunctiva, epithelium, proliferation, wound healing, myofibroblast

Mucins are located at the apical surfaces of all wet-surfaced epithelia and are essential for the homeostasis of these epithelia.[1] They are a class of high-molecular weight hydrophilic glycoproteins and contain multiple tandem repeats of amino acids that are rich in serine and threonine in the central domain of the core peptide.[2] The number of amino acids per tandem repeat varies between each mucin gene.[3] The number of tandem repeats per allele also varies, making these genes and the resultant proteins polymorphic.[3] The abundant O-linked carbohydrate side chains provide the very hydrophilic character of mucins.[4] Epithelial mucins are categorized as secreted and membrane-associated mucins (MAMs). Secreted mucins including MUC5AC have no transmembrane-spanning domains and are produced by goblet cells[5]; they can trap allergens, debris, and pathogens to facilitate their clearance from mucosal surfaces.[6] Membrane-associated mucins, such as MUC1, MUC4, and MUC16 (Muc1, Muc4, and Muc16 in mice), have a short cytoplasmic tail, a single transmembrane domain, an autoproteolytic domain, and a large, heavily glycosylated extracellular domain that contributes to the formation of the glycocalyx of apical cells in wet-surfaced epithelia.[1] The functions of the MAMs include an antiadhesive action, lubrication, water retention, and a pathogen barrier function.[1,7] Recent research has established that mucins exhibit anti-inflammatory effects; MUC1 has reportedly been involved in the regulation of *Haemophilus influenza*–related inflammation.[8] Mucin 2 can play a major role in the development of experimental colitis.[9]

The ocular surface epithelia also express three MAMs, which are concentrated on the tips the apical cells' microplicae and form a dense glycocalyx at the epithelium–tear film interface.[1] Mucin 1 is expressed in both corneal and conjunctival epithelia.[10,11] Mucin 4 is most prevalent in the conjunctival epithelia in humans.[11,12] Mucin 16 (or Muc16 in mice) is expressed in both corneal and conjunctival epithelia in humans,[11,13] but only in the conjunctival epithelia in mice.[14] Membrane-associated mucins that are expressed on the ocular surface may prevent the adhesion of adjacent cell surfaces during blinking or sleeping.[1] The ocular surface of Muc1-null mice with C57BL/6 background appeared normal in all respects tested.[15]

Because MAMs are considered to modulate local tissue inflammation as described above, it is hypothesized that the loss of Muc16 might induce the expression of inflammatory cytokines in mouse conjunctiva and secondarily affect the homeostasis of the corneal epithelium. To explore this hypothesis, we employed Muc16 knockout (KO) mice. Muc16-deficient homozygous mutant mice (KO mice) appeared normal, were fertile, displayed a normal rate of growth, and did not display any abnormal phenotypes.[16] Cheon et al.[16] did not detect any histological differences in the ovary, uterus, lung, or testis between the wild-type (WT) and KO mice. However, our present study demonstrated that the loss of Muc16 in the conjunctiva certainly impaired the homeostasis of the corneal epithelium and stroma.

Materials and Methods

The experimental protocols and use of experimental mice were approved by the DNA Recombination Experiment Committee and the Animal Care and Use Committee of Wakayama Medical University and conducted in accordance with the Association for Research in Vision and Ophthalmology Statement for the Use of Animals in Ophthalmic and Vision Research. Age-matched KO mice with C57BL/6 background and C57BL/6 (WT) mice were used.

Histology

Histology was first carried out in the paraffin sections of WT and KO eyes of 14-day-old ($n = 4$ in each genotype), 56-day-old ($n = 4$ in each genotype), and 6-month-old ($n = 4$ in each genotype) mice. Hematoxylin and eosin (HE) staining and Periodic acid-Schiff (PAS) staining were employed. The number of PAS-positive cells per section of WT and KO eyes of the 56-day-old mice was counted. The 56-day-old adult KO mice ($n = 2$) and WT mice ($n = 2$) were used for the ultrastructure examination. After the WT and KO mice were killed, the eyes were enucleated and fixed with 2% glutaraldehyde in 0.1 M PBS (pH 7.4) for 48 hours. They were postfixed with 1% OsO4 in 0.1 M PBS, dehydrated, and embedded in Epon/Araldite. Ultrathin sections were cut with a diamond knife, attained with uranyl acetate and lead citrate, and observed under transmission electron microscopy as previously reported.[17]

Morphology of the Nuclei of the Corneal Epithelium

Histology suggested that the suprabasal cells of the KO corneal epithelium appeared less flattened compared with those in a WT mouse. Therefore, we examined the shape (the degree of the flatness) of the nucleus in the corneal epithelium of 8-week-old WT and KO mice using 4′,6-diamidino-2-phenylindole (DAPI) staining to analyze the maturation of the suprabasal cells as previously reported.[18] The ratios between the horizontal and vertical lengths of the cell nucleus in the corneal basal cell layers and the suprabasal cell layers were measured as previously reported.[18]

Real-Time Reverse Transcription-Polymerase Chain Reaction (RT-PCR)

We ran RT-PCR for interleukin 6 (IL-6), tumor necrosis factor-α (TNFα), Muc1, Muc4, and Muc5AC in RNA samples from the cornea and conjunctiva (including subconjunctival connective tissue, referred as conjunctiva in the current manuscript) from 8-week-old WT and KO mice ($n = 20$ in each genotype) as previously reported.[19] The primers that were used have been listed in Table 1.

Table 1. Primers and Oligonucleotide Probes Used for Real-Time PCR

Primer	Oligonucleotide Probe
TNFα	Mm00443258_m
IL-6	Mm01210732_gl
Muc1	Mm00449604_m1
Muc4	Mm00466886_ml
Muc5 AC	Mm01276718_ml
ALDH3A1	Mm00839312_ml
αSMA	Mm01204962_gh
GAPDH	Mm03302249_gl

GAPDH, glyceraldehyde-3-phosphate dehydrogenase.

Immunohistochemistry

The paraffin sections (5 μm thick) of the 8-week-old mouse eyes were deparaffinized, rehydrated, and subjected to immunohistochemistry for phospho-Stat3, AP-1 components (c-Fos, c-Jun, JunB, and JunD), IL-6, keratin 12 (K12), and keratin 14 (K14) as previously reported.[18] The antibodies that were used have been listed in Table 2. The paraffin sections (5 μm thick) of the 2-week-old and 6-month-old mouse eyes were subjected to immunohistochemistry for phospho-Stat3 and K14. After the primary antibody reaction and washing in PBS, the specimens were allowed to react with peroxidase-conjugated polyclonal secondary antibodies (1:200 in PBS; Cappel, Organon-Teknika, West Chester, PA, USA). After washing in PBS, the reaction was visualized with 3,3′-diaminobenzidine (DAB) as previously reported,[20] and the sections were counterstained with methyl green and mounted in balsam. Negative control staining was performed by the omission of each primary antibody and did not yield specific staining (not shown).

5-Bromo-2′-Deoxyuridine (BrdU) Immunolabeling

To examine the patterns of DNA replication (cells in S-phase of the cell cycle), the incorporation of BrdU was analyzed using immunohistochemistry as previously reported.[21] The WT and KO eyes of 2-week-old ($n = 3$ in each genotype), 8-week-old ($n = 8$ in each genotype), and 6-month-old ($n = 3$ in each genotype) mice were used. The mice were intraperitoneally

Table 2. Antibodies Used for Immunohistochemistry

Antibody	Host	Company	Dilution
Muc16(C-6)	Mouse	Santa Cruz Biotechnology, Santa Cruz, CA, USA	×50
Phospho Stat3(B7)	Mouse	Santa Cruz Biotechnology	×50
c-Fos(Ab-2)(4-17)	Rabbit	Calbiochem, San Diego, CA, USA	×100
c-Jun/AP-1(Ab-3)	Mouse	Calbiochem	×50
JunB	Rabbit	Atlas Antibodies AB, Stockholm, Sweden	×50
JunD	Rabbit	Biorbyt Limited, Cambridge, Cambridgeshire, UK	×100
IL-6(M-19)-R	Rabbit	Santa Cruz Biotechnology	×200
F4/80	Mouse	BMA Biomedicals, Augst, Switzerland	×50
αSMA	Mouse	Neomarker, Fremont, CA, USA	×200
ALDH3A1(G-2)	Mouse	Santa Cruz Biotechnology	×100

Antibodies were diluted in PBS.

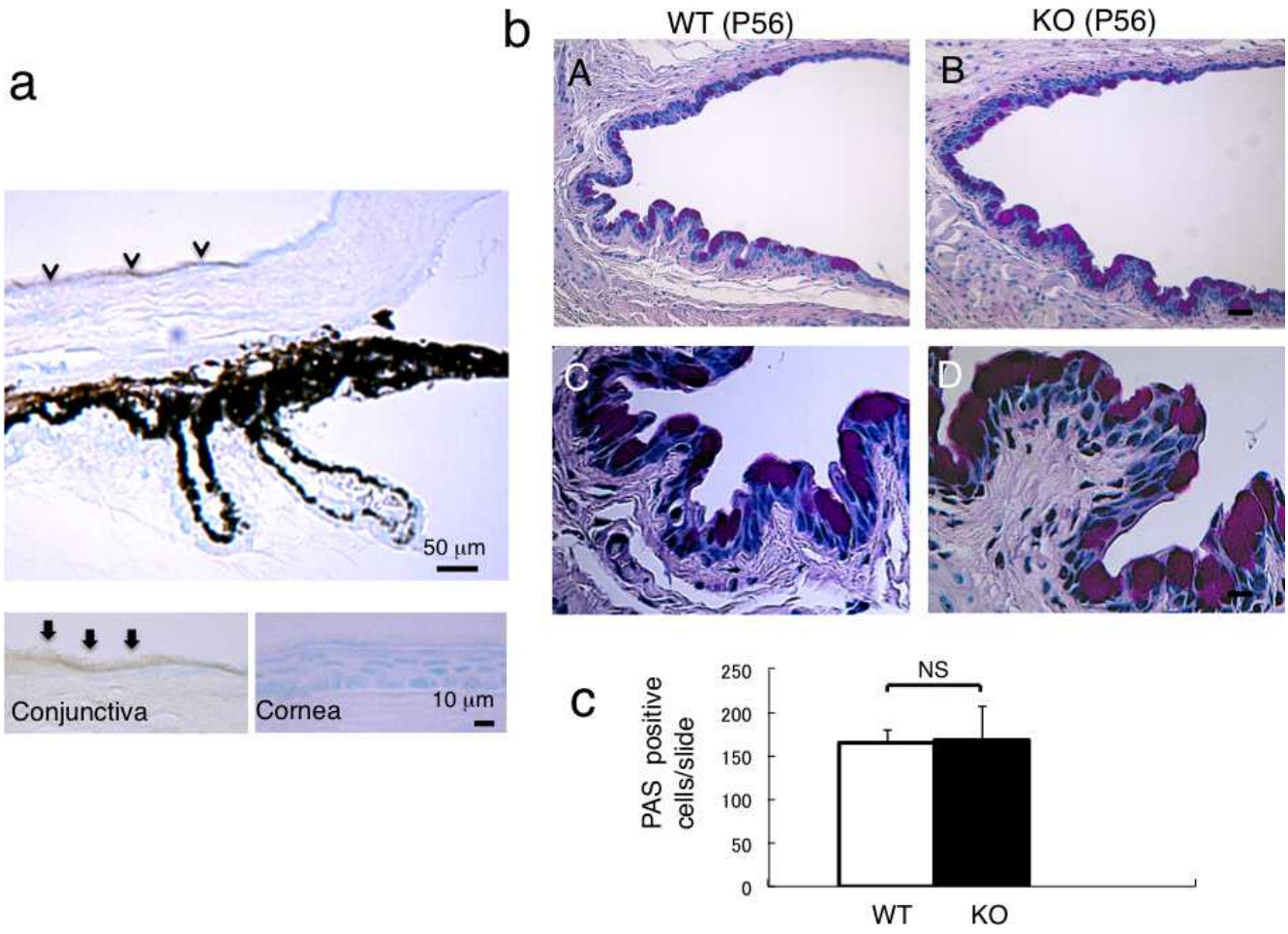

Figure 1. Expression of Muc16 in mouse ocular tissues and the histology of conjunctiva of WT and KO tissues. (**a**) Mucin 16 is expressed in conjunctival epithelium, but not in corneal epithelium. Higher magnification picture (*insert*) shows Muc16 in the superficial layer of the conjunctival epithelial cells. (**b**) Histology by PAS staining shows no obvious difference in the morphology of the conjunctival epithelium between WT (**A**) and KO (**B**) mouse. *Scale bar*: 50 μm. Higher magnification observation did not indicate differences in the morphology of goblet cells between WT (**C**) and KO (**D**) mouse. *Scale bar*: 10 μm. (**c**) The number of goblet cells was not affected by the loss of Muc16.

injected with 1 mL/100 g BrdU (Amersham, Buckinghamshire, UK), and 2 hours later, the animals were killed, and the eyes were enucleated. The eyeballs were fixed in 4% paraformaldehyde and embedded in paraffin. The specimens were cut at 5-μm thickness. Five sections per eyeball were used to BrdU staining. The interval between the sections was at least 25 μm. Deparaffinized sections were treated with 2 N HCl for 1 hour at 37°C and then washed in PBS before the application of the antibody. The mouse monoclonal anti-BrdU antibody (1:10; Roche Diagnostics, Mannheim, Germany) was diluted in PBS. After DAB reaction (according to the manufacturer's protocol), methyl green counterstaining, and mounting, the number of BrdU-positive cells in the corneal epithelium per section were counted.

TUNEL Assay

We carried out TUNEL assay in the deparaffinized sections (5-μm thick) of the 8-week-old mouse eyes as previously reported.[22] In brief, sections were digested by with proteinase K (10 μg/mL; Sigma-Aldrich, St. Louis, MO, USA) for 5 minutes at room temperature. After washing, the sections were treated with 1 × TdT buffer containing TdT (Invitrogen, CA, USA) and biotinylated-dUTP (Roche Diagnostics, Mannheim, Germany) for 45 minutes at 37°C. After the sections were washed with PBS, a reaction with streptavidin-peroxidase and DAB reaction was performed. After counterstaining with methyl green, the sections were mounted in balsam. For a negative control, specimens were stained without the biotinylated-dUTP. For a positive control, the sections were treated with 10 μg/mL of DNase I for 10 minutes and then examined.

Wound Healing of Corneal Epithelial Defect

Adult 8-week-old KO mice ($n = 6$) and WT mice ($n = 6$) were used. A round corneal epithelial defect (diameter: 2.0 mm) was made with a 2-mm trephine and a scalpel in the right eye. This procedure left the basement membrane intact. The affected corneas were stained with fluorescein and photographed under a microscope at 0, 6, 12, 18, 24, and 30 hours after injury. The fluorescein-stained areas of the epithelial defect were measured from photographs obtained under the microscope. At 30 hours post debridement, the numbers of the corneas with or without stromal opacification (scar) were statistically analyzed using the χ^2 test. Each eye was then processed for histology and immunohistochemistry for α-smooth muscle actin (αSMA), aldehyde dehydrogenase 3A1 (ALDH3A1), and F4/80 macrophage antigen as described above.[20] The antibodies that were used have been listed in Table 1.

Investigative Ophthalmology & Visual Science

Another set of corneas that were healing post debridement from 8-week-old WT and KO mice ($n = 10$ each) were processed for RNA extraction and real-time PCR for mRNAs of αSMA and ALDH3A1 as previously reported.[19] We used a real-time PCR system (TaqMan; Applied Biosystems, Forest City, CA, USA) as described above. The primers that were used have been listed in Table 1.

Statistical Analysis

The statistical analysis in each experiment except for the evaluation of corneal opacification was performed using unpaired *t*-tests. A value of $P < 0.05$ was considered statistically significant.

Results

Expression of Muc16 in a WT Mouse Eye

Mucin 16 proteins were detected in the superficial epithelial cells in the conjunctiva and were not detected in the cornea in the WT mice (Fig. 1a).

Gross Appearance and Histology of the Cornea of a KO Mouse

Under biomicroscopy, eyes appeared normal in both WT and KO mice (Figs. 2A, 2B). The corneal surface of both WT and KO mice were quite normal and similar to each other with only very minor punctate fluorescein staining (detailed data not shown). We then examined the histology of the conjunctiva using PAS staining because Muc16 is a conjunctiva-specific MAM in mice. We found no difference in the structure of the conjunctival epithelium and the numbers of goblet cells between WT and KO mice (Figs. 1B, 1C). Histology by HE staining showed that the thickness of the stratified epithelium of the cornea appeared normal in KO mice compared with WT mice corneal epithelium. The suprabasal epithelial cells were relatively round or less flattened in the KO corneal epithelium compared with the WT corneal epithelium (Figs. 2C, 2D). Scanning electron microscopy also did not demonstrate a significant difference in the features of the surface of the superficial corneal epithelium between WT and KO mice (data not shown).

To further observe the structure of the basal and suprabasal cells in the corneal epithelium, transmission electron microscopy was performed. Ultrastructural observation showed that suprabasal cells seemed to have a similar size as that of basal cells in the KO corneal epithelium, whereas the size of suprabasal cells seemed smaller than that of the basal cells in the WT mouse (Figs. 2E, 2F). More nuclei were observed in the superficial layer of the KO cornea than in the WT cornea. Mitotic cells were seen more frequently in the KO corneal epithelium than in the WT corneal epithelium. The morphology of the microplicae of the superficial cells of the epithelium did not seem to be affected by the loss of Muc16 under transmission electron microscopy (data not shown).

Expression Pattern of Phospho-Stat3 and AP-1 Components in WT and KO Cornea and Conjunctival Tissues

Immunoreactivity for phospho-Stat3 was not observed in the corneal epithelium and keratocytes of both WT and KO mice as well as in the WT conjunctiva. However, marked phospho-Stat3 immunoreactivity was detected in fibroblasts in the subconjunctival connective tissue of KO mice (Fig. 3a). Immunoreactivity for c-Fos or c-Jun was not observed in the corneal epithelium and was very faintly seen in the conjunctival epithelium of both WT and KO mice (data not shown). While JunB protein was observed in some basal cells of the WT and KO corneal epithelia and in the WT conjunctival epithelium, it was detected in the superficial epithelial cells in the KO conjunctiva (Fig. 3b). JunD protein was observed in the basal cells of the WT and KO corneal and conjunctival epithelia, and the distribution of labeled nuclei seemed similar (Fig. 3c).

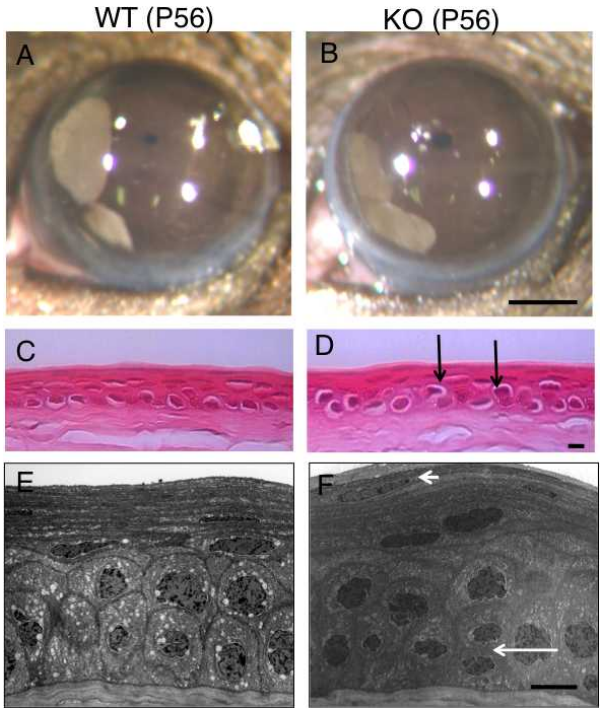

Figure 2. Histology of WT and KO cornea. No obvious opacification or other epithelial disorders were observed in both WT (**A**) and KO (**B**) mouse corneas. *Scale bar*: 1 mm. Hematoxylin and eosin histology shows that the thickness of the stratified epithelium of the cornea seems normal in the KO mouse (**D**) compared with the WT mouse corneal epithelium (**C**). The suprabasal epithelial cells (*arrows*) were relatively round or less flattened in the KO corneal epithelium compared with these cell types in the WT cornea. Ultrastructural observation showed that the size of suprabasal cells seemed similar to that of basal cells in the KO corneal epithelium (**F**), while the size of the suprabasal cells looked smaller than that of the basal cells in the WT mouse (**E**). More nuclei were observed in the superficial layer of the KO cornea compared with the WT mouse (*small arrow*). Mitotic cells were more frequently seen in the KO epithelium compared with the WT cornea (*large arrow*). *Scale bar*: 10 μm.

Effects of the Loss of Muc16 on the Expression of Mucin Genes and IL-6, TNFα in Ocular Surface Epithelia

We first examined if the loss of Muc16 was compensated by the upregulation of other mucins using real-time PCR. The expression of Muc1 mRNA was higher and the expression of Muc4 mRNA was lower in conjunctiva than in the cornea (Fig. 4d). There was no statistical difference in the expression levels of Muc1 and Muc4 between the WT mice and KO mice. The expression of Muc5AC gene in the conjunctiva was not affected by the loss of Muc16 gene (Fig. 4d).

We detected the upregulation of phospho-Stat3 in the KO subconjunctival fibroblasts in vivo, which prompted us to hypothesize that the expression of inflammatory mediators

Investigative Ophthalmology & Visual Science

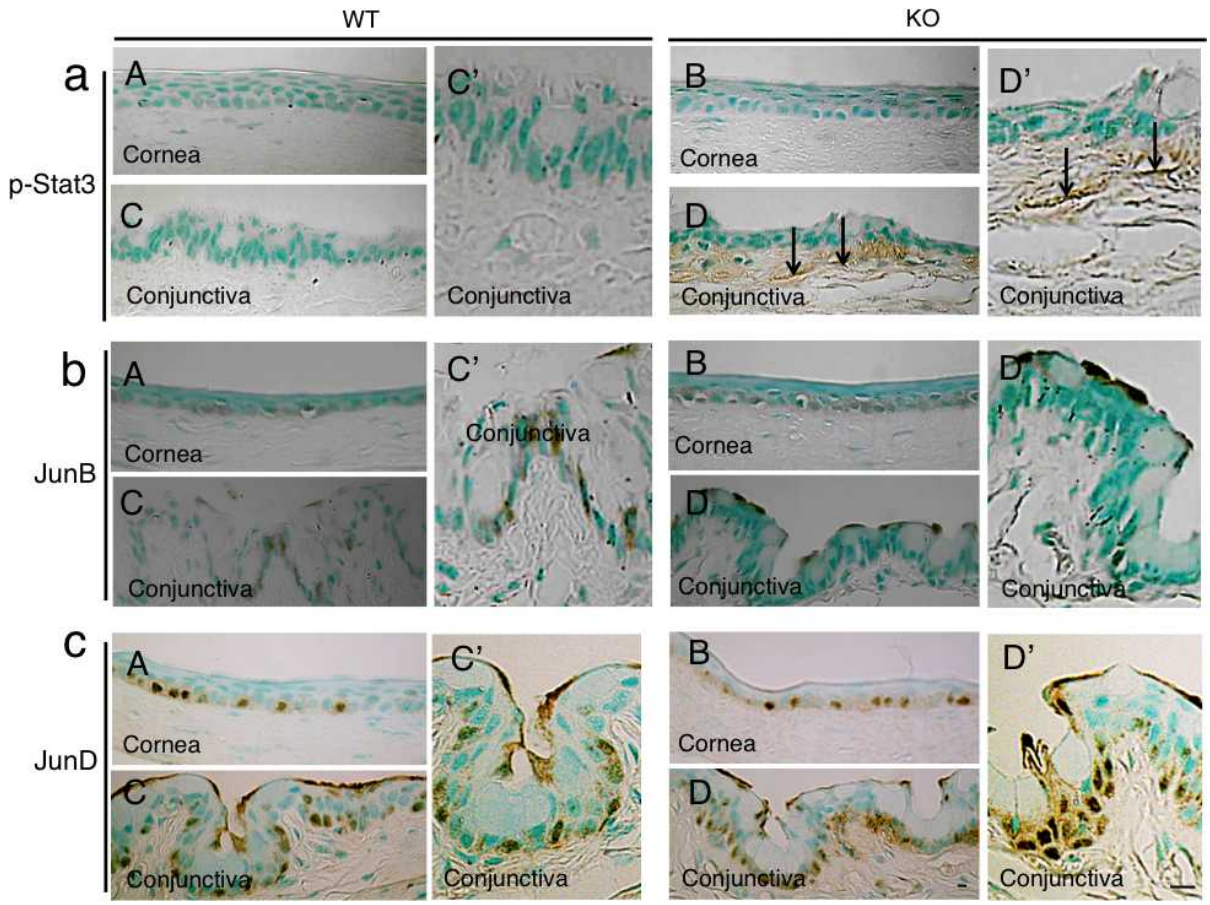

Figure 3. Expression pattern of phospho-Stat3 and AP-1 components in ocular surface. (**a**) Phospho-Stat3 was detected in subepithelial fibroblasts (*arrows*) in the KO conjunctiva ([**D**], higher magnification in [**D**']), but was not seen in the WT tissue ([**C**], higher magnification in [**C**']), as well as in the corneal epithelium and keratocytes in both genotypes of mice (**A**, **B**). (**b**) JunB protein was observed in some of the basal cells of WT and KO corneal epithelia (**A**, **B**) as well as in WT conjunctival basal epithelial cells ([**C**], higher magnification in [**C**']), while it was detected in the superficial epithelial cells in KO conjunctiva ([**D**], higher magnification in [**D**']). (**c**) Nuclear JunD is restricted to the basal layer cells of both the cornea and conjunctiva in both genotypes of mice (**A**–**D**). *Scale bar*: 10 μm.

might be expressed in the cells. To test this possibility, several real-time PCR evaluations for the mRNAs of IL-6 and TNFα were completed. The expression of TNFα mRNA was not affected by the loss of Muc16 in each of cornea or conjunctiva (Fig. 4a). The loss of Muc16 did upregulate the expression of IL-6 mRNA in the conjunctiva ($^*P < 0.05$), but not in the cornea (Fig. 4b). To examine if the findings would be the same with protein expression, we conducted immunohistochemistry for IL-6 in the WT and KO ocular tissues. The results showed that the expression of IL-6 protein was faintly detected in basal cells of the corneal epithelium and detected in the subconjunctival connective tissue of both WT and KO mice (Fig. 4c). Although immunohistochemistry is a qualitative but not quantitative analysis, the immunoreactions in subconjunctival tissue appeared more marked in the KO tissue compared with the WT tissue.

Evaluation of the Morphology of the Nuclei of the Corneal Epithelium and Expression of K12 and K14

These morphological findings suggested that the intraepithelial cell differentiation, such as the differentiation of a basal-type cell to a suprabasal-type cell, might be impaired. To explore this hypothesis, we then tried to test this process by evaluating the morphology of the nuclei of basal and suprabasal cells in each genotype of the epithelium with DAPI nuclear staining (Fig. 5a) as previously reported.[18] We calculated the ratio of the horizontal length to the vertical length of the nucleus (Fig. 5b). The ratio of the horizontal to the vertical length of the nucleus in the corneal basal cell layers was 1.99 ± 0.55 in WT mice and 1.28 ± 0.40 in KO mice ($P < 0.005$) (Fig. 5c). The ratio in the corneal suprabasal cell layers was 2.90 ± 0.63 in WT mice and 1.79 ± 0.47 in KO mice ($P < 0.001$; Fig. 5c). In both the basal cells and suprabasal cells, the nuclei of the KO mice were relatively more round in shape in the sections compared with the WT cells.

The marker of corneal epithelium, K12, was detected in the corneal epithelial cells, and was more intense in the basal layer cells, of both the WT mice and KO mice (data not shown). This indicated that the loss of Muc16 in the conjunctival epithelium did not affect the cornea-type epithelial differentiation. A specific keratin of the basal cells of stratified epithelia, K14, was detected in the basal cells of the corneal epithelium of the WT mice. However, it was observed in the basal cells and the cells upon the basal cells of the corneal epithelium of the KO mice (Fig. 5d).

Cell Proliferation and Apoptosis in the Corneal Epithelium of a KO Mouse

Cells that were BrdU-positive were scattered throughout the basal layer of the corneal epithelial cells of the WT mice and

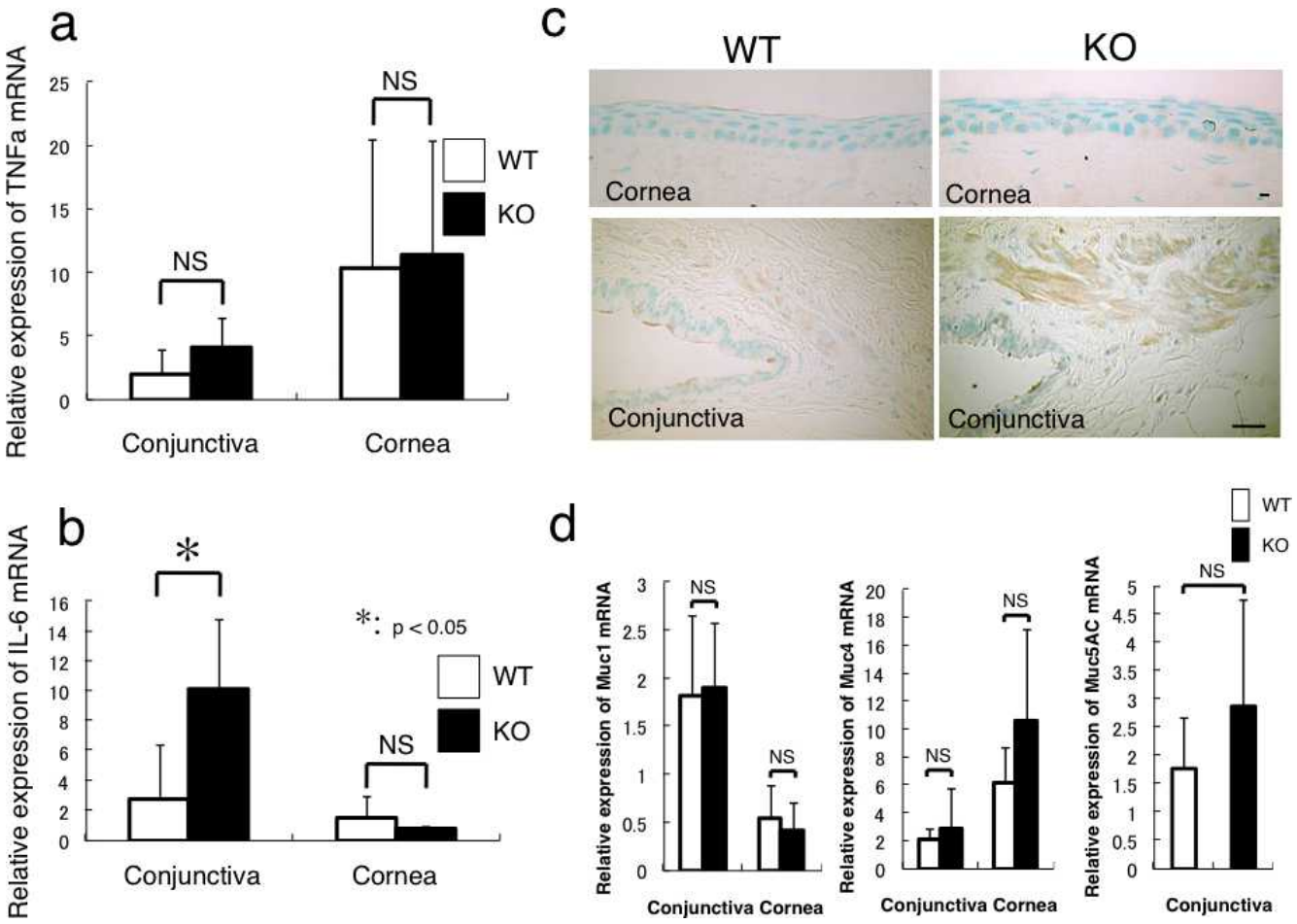

Figure 4. Expression of inflammatory components and membrane-associated mucin family members in cornea and conjunctiva. (**a**) Real-time reverse PCR clearly shows that there is no statistical difference in the expression level of TNFα mRNA between WT and KO mice in conjunctiva or cornea. (**b**) The loss of Muc16 promotes the mRNA expression of IL-6 in the conjunctiva (*$P < 0.05$), but not in the cornea. (**c**) Immunohistochemistry for IL-6 suggests that the subconjunctival tissue, but not the cornea, is the main source of IL-6 in the ocular surface in both genotypes of mice, and that IL-6 immunoreactivity seems more intense in the KO tissue compared with the WT one. *Scale bar*: 10 μm (cornea); 50 μm (conjunctiva). (**d**) The mRNA expression of Muc1 or Muc4 is higher in the conjunctiva or cornea, respectively, but there is no statistical difference in their expression levels between WT and KO tissues. The expression of Muc5AC mRNA in the conjunctiva is not significantly affected by the loss of Muc16.

KO mice (Fig. 6a). In the 8-week-old mice, BrdU-positive cells were more frequently observed per section in the KO mice compared with the WT mice; the number of cells was 13.85 ± 5.68 in WT mice and 16.93 ± 6.30 in KO mice ($P < 0.05$; Fig. 6b).

We attempted to detect apoptotic cells using TUNEL staining. Cells that were TUNEL-positive were not detected in the corneal epithelial cells of the WT and KO mice (Fig. 6c).

Age-Dependency of KO Phenotype

To determine if the abnormality in the cornea and conjunctiva in a KO mouse was age-dependent, we investigated the morphology and proliferation activity of the corneal epithelium and the expression of pStat3 in the cornea and conjunctiva of 2-week- and 6-month-old WT and KO mice as described above. The corneal epithelium of the 2-week-old mice displayed one or two layers. The histology of conjunctival and corneal epithelia was similar between 2-week- or 6-month-old WT and KO mice (Fig. 7a). Keratin 14 was detected in the basal cells of the corneal epithelium of the WT and KO mice (Fig. 7a). A few suprabasal cells were labeled for K14 in the corneal epithelium of 2-week- or 6-month-old WT and KO mice. The expression of phospho-Stat3 was not detected in the epithelium and stroma of the WT and KO cornea of the 2-week-old mice. In contrast, pStat3 immunoreactivity was detected in the fibroblasts in the subconjunctival connective tissue of the 6-month-old KO mice (Fig. 7a). There was no statistical difference in the number of BrdU-positive cells/section between the 2-week- or 6-month-old WT mice and KO mice (Fig. 7b).

Wound Healing of the Cornea Following Epithelial Debridement

The corneal epithelial wound closure was determined by the disappearance of the fluorescein-stained epithelium in the areas of defects. The areas with the epithelial defects healed faster in the KO mice compared with the WT mice (Fig. 8a). The wound area at 12 hours was 1.91 ± 0.16 mm^2 in the WT mice and 1.60 ± 0.27 mm^2 in the KO mice ($P < 0.05$). The wound area at 12 hours was significantly decreased in the KO mice (Fig. 8b). At 30 hours post debridement, all but one of the WT corneas were without stromal opacification (scar), while all six corneas exhibited stromal opacification in the KO mice

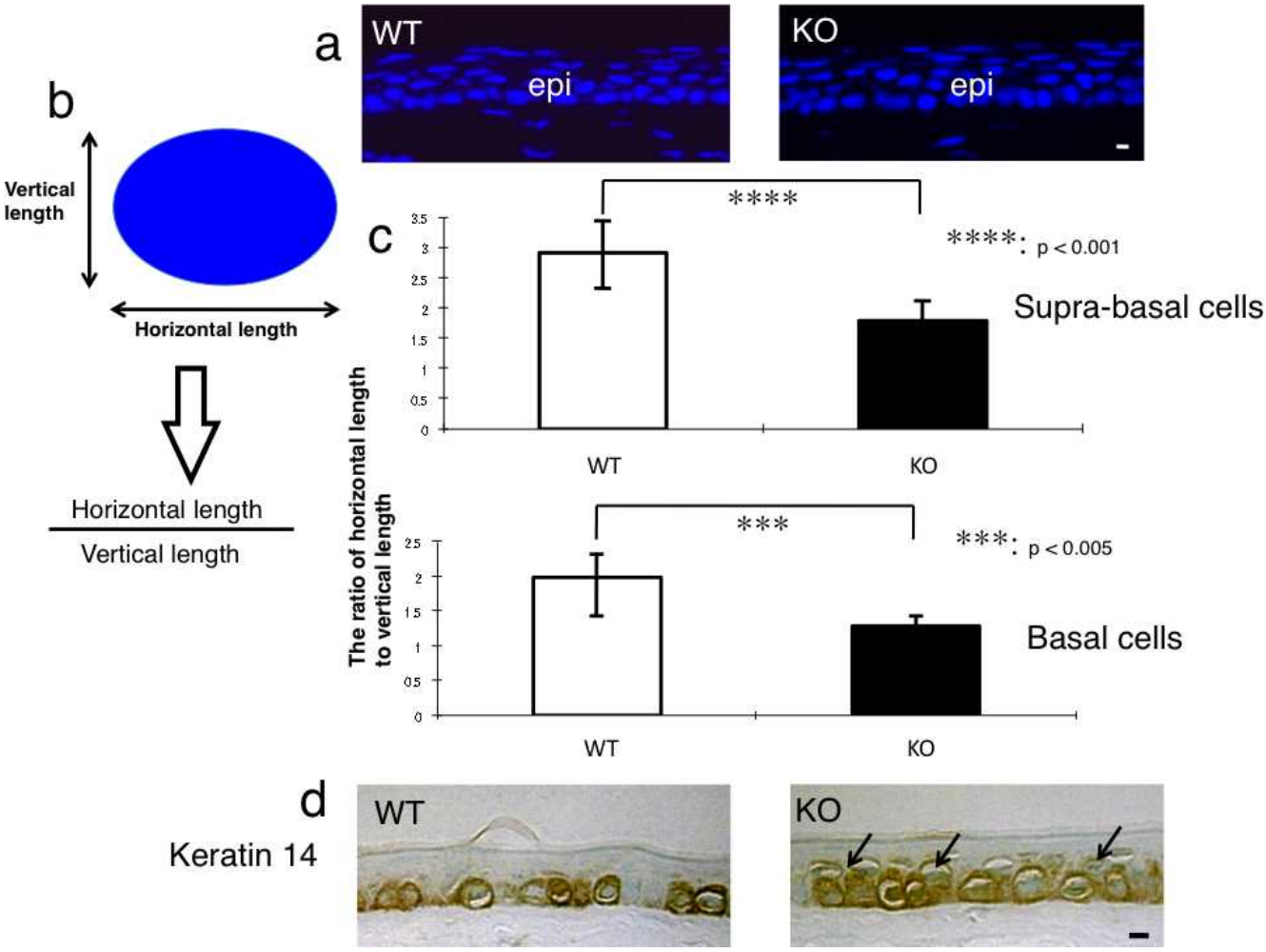

Figure 5. Evaluation of intraepithelial differentiation of the corneal epithelium. (**a**) In order to evaluate the morphology of the nuclei of the basal and suprabasal cells of the corneal epithelium, the tissue was stained with DAPI nuclear staining. *Scale bar*: 10 μm. (**b**) The ratio of horizontal/vertical length of the nucleus of suprabasal or basal cell was calculated to evaluate the intraepithelial differentiation of an epithelial cell. (**c**) The ratio of horizontal/vertical length of the nuclei of suprabasal cells and of basal cells was significantly lower in the corneal epithelium of the adult KO mice than in adult WT mice. ***$P < 0.005$ and ****$P < 0.001$ by unpaired Student's *t*-test. *Bar*: standard error. (**d**) Keratin 14, a marker of basal epithelial cells, was detected in the basal cells of the corneal epithelium of a WT mouse, while both basal and suprabasal cells (*arrows*) were labeled for keratin 14 in the corneal epithelium of a KO mouse. *Scale bar*: 10 μm.

(Fig. 8a). The data were statistically analyzed and we found that the incidence of corneal stromal opacification in the KO mice was statistically ($P < 0.01$) higher than in the WT mice.

Immunohistochemistry showed that F4/80-labeled macrophages were found in the subepithelial layer of the KO corneas at 30 hours post debridement, while few F4/80-labeled cells were seen in the WT corneas (Figs. 9aA, 9aB). The cells in the posterior stroma were labeled for ALDH3A1, and thus showed the keratocytic phenotype, while the fibroblastic cells in the anterior stroma were not labeled in the WT cornea (Fig. 9aC). In the KO cornea, the majority of the cells in the stroma were negative for ALDH3A1 (Fig. 9aD). The majority of keratocytes in the KO corneas were labeled with anti-αSMA antibody while the stromal cells in the WT mice were minimally positive for αSMA (Figs. 9aE, 9aF). The immunohistochemical findings of phenotypic alterations in the keratocytes were not observed in the stroma of the peripheral cornea (data not shown). Real-time PCR indicated no difference in the mRNA expression levels of ALDH3A1and αSMA (Figs. 9b, 9c).

Discussion

The present study demonstrated that the loss of a MAM member, Muc16, affected the homeostasis of the ocular surface epithelium in mice. The loss of a conjunctiva-specific mucin significantly impaired the homeostasis of not only conjunctival but also corneal epithelium. As mentioned in the introduction, the expression pattern of Muc16 (or MUC16 in humans) differs between mice and humans; it is expressed in both cornea and conjunctiva epithelia in humans,[11,13] but only in the conjunctiva in mice.[14] However, the present findings clearly indicated that MAM expression in the conjunctiva was essential to maintain ocular surface homeostasis; this is an important concept to understand the disease mechanism underlying human dry eye patients.

First, we showed that the loss of Muc16 activated Stat3 signal in the subconjunctival tissue and upregulated the expression of IL-6 in conjunctiva (including subconjunctival connective tissue); this suggested that the loss of Muc16 might induce a subclinical inflammatory reaction without additional

Investigative Ophthalmology & Visual Science

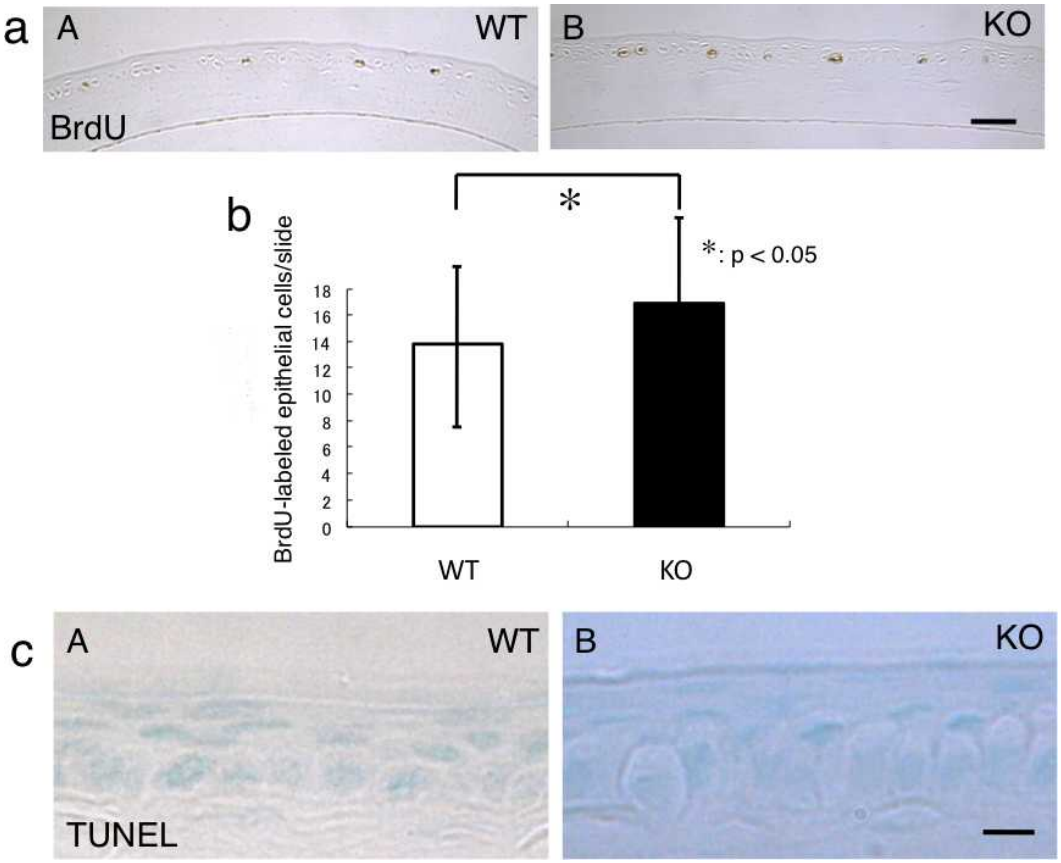

Figure 6. Proliferation activity and apoptosis in corneal epithelium. (**a**) The presence of proliferating cells was detected by BrdU labeling. BrdU-labeled cells were observed in the basal layer of the corneal epithelium of both genotypes (**A**, **B**). *Scale bar*: 50 μm. (**b**) The number of BrdU-labeled cells in each cornea section was higher in the KO mouse than in the WT tissue. $^*P < 0.05$. (**c**) TUNEL-labeled apoptotic cells were not detected in the corneal epithelia of both WT (**A**) and KO (**B**) mice. *Scale bar:* 10 μm.

external stimuli. Although there was no difference in the activation level of JunD signal, it has also reportedly been involved in the promoter activity of IL-6.[23] Several studies have reported that MAM members demonstrated anti-inflammatory activity in organs other than the eye,[8,9] which supports the current findings, although the exact mechanism how the loss of Muc16 modulates Stas3 signaling and the expression of IL-6 in conjunctiva is still unknown. A MAM member, Muc13, reportedly exhibited anti-inflammatory activity in the mouse intestine; the loss of Muc13 caused spontaneous focal inflammation as well as exaggerated dextran sodium sulfate-induced colitis in mice.[24] Muc1-deficient tissue of the gastrointestinal tract or intestinal epithelial cell line with Muc1-silencing increased the chemokine expression in response to the exposure to TNFα in culture.[25] Although data that demonstrates that Muc16 possesses a similar anti-inflammatory activity are unavailable, our current data indicated that Muc16 could modulate tissue inflammation in vivo in the mouse conjunctiva. On the other hand, Muc16 may provide a protective barrier for the epithelial surface from bacterial adherence and to suppress the immune system by suppressing the activity of natural killer cells.[26] For example, the knockdown of Muc16 in cultured human corneal limbal epithelial cells promoted the adhesion of bacteria on the cell surface.[27] Therefore, the loss of Muc16 in conjunctiva may have disrupted the normal relationship between the tissue and commensal bacteria. To further characterize the relationship between Muc16-null conjunctiva and bacterial components, the effects of the topical administration (eye drop or subconjunctival injection[28,29]) of commercially available lipopolysaccharides on signal transduction and on gene expression pattern need to be examined.

The loss of Muc16 also affected the activation status of the AP-1 components in the conjunctival epithelium, although its biological importance has not been determined. The expression pattern of JunB, but not c-Fos, c-Jun, and JunD, in the conjunctival epithelium was altered by the loss of Muc16. Although the mechanism for the alteration of AP-1 components by Muc16 gene ablation in the conjunctival epithelium still has to be investigated, a similar expression pattern was reported in an inflamed human skin sample: the epidermis of a skin biopsy specimen from a patient with systemic lupus erythematosus showed a decreased level of JunB and the activation of Stat3 in association with dermal IL-6 upregulation.[30]

Dry eye is a multifactorial ocular surface disorder that causes ocular dryness, discomfort, pain, and visual disturbance. Tears consist of watery and mucous components as well as those secreted by the Meibomian glands. Although these components are essential to the ocular surface homeostasis, the mechanisms of the development of dry eye syndrome are not fully understood.

Interleukin 6 and mucin genes are upregulated in the conjunctiva of dry eye patients,[31] and IL-6 stimulates the expression of Muc4 in a cultured cell line.[32] However, in the current study, we did not observe a significant alteration of the expression level of other mucins (i.e., Muc1, Muc4, and Muc5Ac). We then considered that the upregulation of IL-6 in the conjunctiva might affect the homeostasis of the corneal

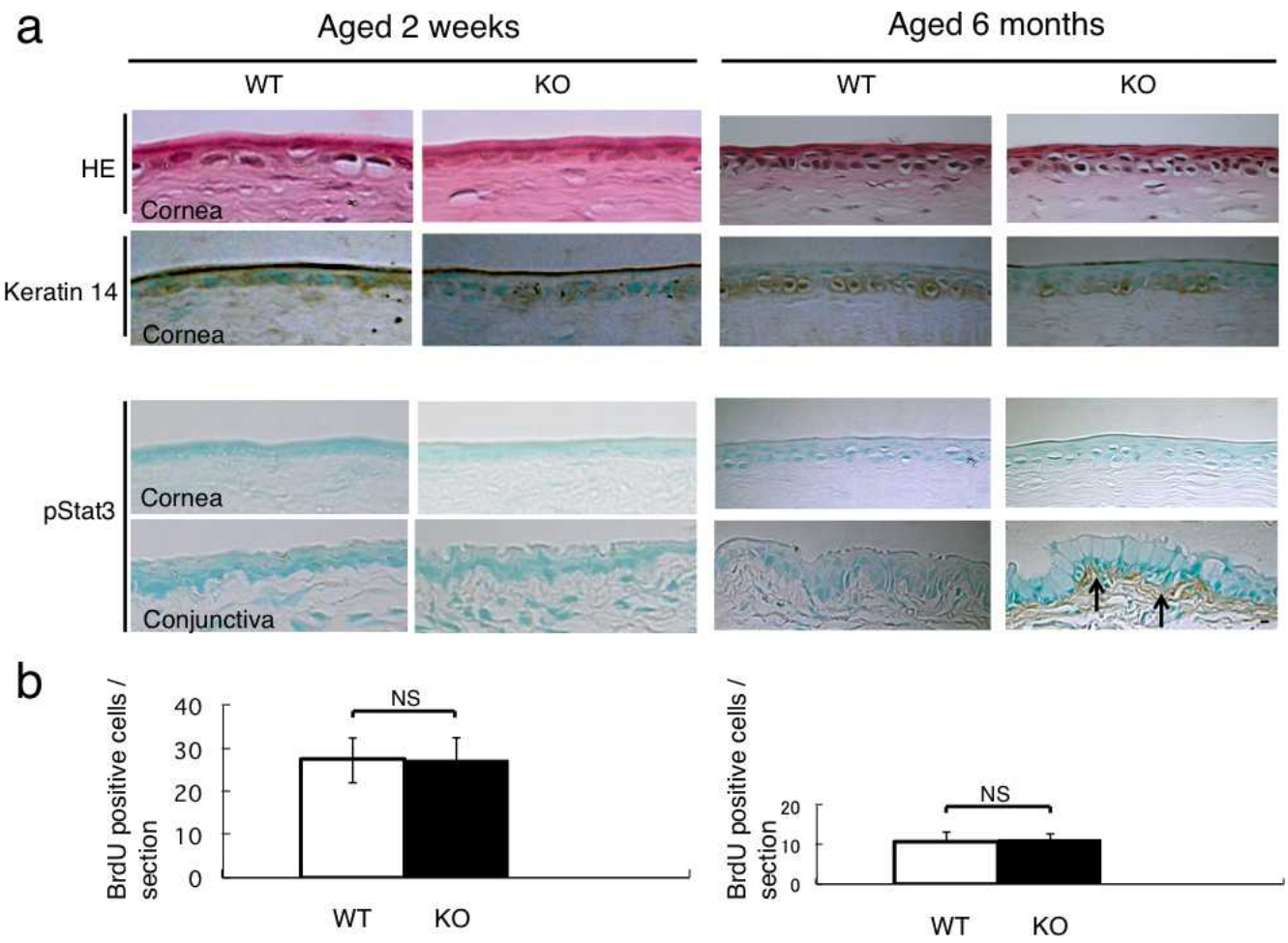

Figure 7. Corneal epithelium and conjunctiva of 2-week-old and 6-month-old mice. (**a**) Hematoxylin and eosin staining histology and the expression pattern of keratin 14 were similar between WT and KO mice at the ages of two weeks and six months. The corneal epithelium was negative for phospho-Stat3 in both WT and KO mice at the ages of 2 weeks and 6 months. Subconjunctival cells of the 2-week-old WT and KO mice were negative for pStat3. On the other hand, subconjunctival cells of the 6-month-old KO mouse were labeled for pStat3 (*arrows*), but not in WT tissue. (**b**) The incidence of BrdU-incorporated cells in the corneal epithelium was similar between the WT and KO mice at the ages of 2 weeks and 6 months. *Scale bar*: 10 μm.

epithelium presumably via tears, because IL-6 reportedly stimulated cell migration in the corneal epithelium.[33] It was reported that IL-6 did not affect the proliferation of rabbit corneal epithelial cells in culture, but did enhance the keratinocyte proliferation.[34] Its effects on proliferating activity in mouse corneal epithelium have not been studied. Namely, we first hypothesized that the loss of Muc16 in conjunctiva affected the turnover of the cells in the stratified epithelium of the cornea possibly via the upregulation of IL-6 in the conjunctiva. The corneal surface of both WT and KO mice were similar to each other with only minor punctate fluorescein staining (data not shown). Scanning electron microscopy also did not demonstrate significant differences in the features of the surface of the superficial corneal epithelium between the WT and KO mice (data not shown). Our histological observations by light and electron microscopy suggested the presence of basal cell-like cells in the suprabasal layer of the corneal epithelium in the absence of Muc16. The relatively more round nuclei, as observed using light and electron microscopies and the evaluation of the morphology of the nucleus with DAPI nuclear staining, were detected in the suprabasal layer of the KO epithelium compared with the WT epithelium. Our hypothesis was further confirmed by the immune-detection of K14, a marker of a basal cell of stratified epithelia, in the suprabasal cells. The expression of K12, a marker of cornea-type epithelial differentiation, was not affected by the loss of Muc16. This finding prompted us to hypothesize that either the maturation of a basal cell to a suprabasal cell might be delayed or such maturation might not catch up to the turnover of the cells in the stratified epithelium. In order to validate these hypotheses, we then examined cell proliferation and cell death (apoptosis) in the KO epithelium. The incorporation of BrdU in the basal layer cells was more frequent in the corneal epithelium of the KO mouse compared with the WT epithelium. On the other hand, increased cell proliferation did not increase the epithelial thickness. Thus, we evaluated the cell death in the superficial layer of the corneal epithelium; TUNEL-labeled cells were not seen in both WT and KO epithelia in the current study. However, the presence of TUNEL-labeled cells in the superficial layer of corneal epithelium remains controversial.[35–37] One explanation is that apoptotic cells might be desquamated, and therefore, histology did not pick these TUNEL-labeled cells in the epithelium.

We also investigated if the abnormality of the ocular surface in KO mice depended on the age of the animals. In contrast with the adult 8-week-old mice, the distribution of K14-labeled cells in corneal epithelium was similar between WT and KO

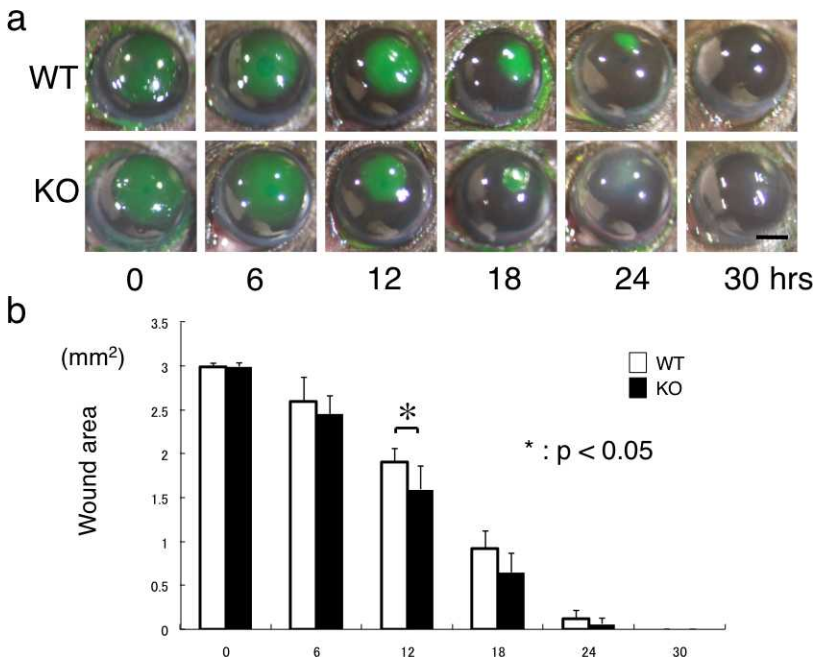

Figure 8. Wound healing of debridement of corneal epithelium. (**a**) The round epithelial defect (stained with green fluorescein) produced in the center of the cornea gradually recovered with the migrating remaining epithelium from outside the defect. In 30 hours post wounding, the defect was closed in both WT and KO mice. The healing rate of the corneal epithelial defect in the KO mouse seemed faster overall compared with the WT mouse. At 24 and 30 hours, the corneal stroma of the area of the regenerated epithelium was transparent in the WT mouse, while it seemed opaque in the KO mouse. *Scale bar*: 1 mm. (**b**) The size of the remaining defect was significantly smaller in the KO mouse cornea compared with the WT cornea at 12 hours post wounding. $^*P < 0.05$. *Bar*: standard error.

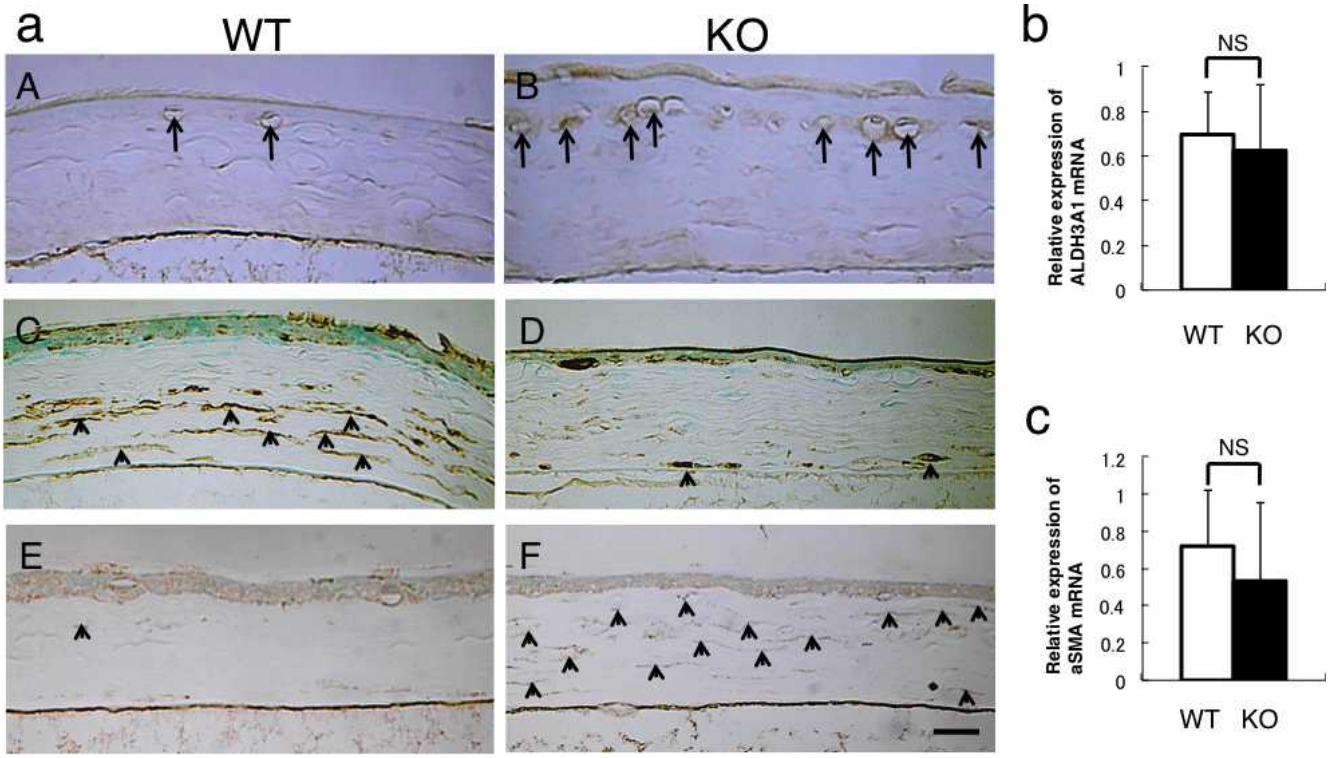

Figure 9. Immunohistochemical detection of macrophages and analysis of keratocyte phenotype in the healed cornea at 30 hours post debridement. (**a**) Immunohistochemistry detects F4/80-labeled macrophages, ALDH3A1 (keratocyte marker), and αSMA (myofibroblast marker). F4/80-labeled macrophages were more frequently observed beneath the regenerated epithelium in the KO mouse (**B**) compared with the WT cornea (**A**). The cells in the posterior stroma were labeled for ALDH3A1, while fibroblastic cells in the anterior stroma were not labeled in the WT cornea (**C**). In the KO cornea, the majority of the cells in the stroma were negative for ALDH3A1 (**D**). A few α-smooth muscle actin–positive myofibroblasts were detected in the WT stroma (**E**). Almost all the stromal cells were labeled with anti-αSMA antibody and thus were myofibroblasts in the KO cornea (**F**). *Scale bar*: 50 μm. Real-time PCR indicated no difference in the mRNA expression level of ALDH3A1 (**b**) and αSMA (**c**).

Investigative Ophthalmology & Visual Science

mice aged 2 weeks and 6 months. The activation of Stat3 was readily observed in the subconjunctival tissue of 6-month-old mice, but not in 2-week-old mice, suggesting that the effects of eyelid opening, such as the colonization of commensal bacteria, might affect Stat3 signal level in the tissue. The incidence of BrdU-labeled epithelial cells in the cornea was not affected by the loss of Muc16 in both 2-week- and 6-month-old mice. The exact reason why the proliferation of corneal epithelium was promoted at age 8 weeks but not at 6 months is unknown. Explanations for this finding might include that the proliferation activity in the corneal epithelium might decrease along with aging.[38]

Interleukin 6 reportedly accelerates the migration of corneal epithelium as revealed by an organ culture experiment.[33] Therefore, the migration of the corneal epithelium following an epithelial defect might be stimulated in the KO mouse compared with the WT mouse. To check this point, we performed a debridement wound healing experiment in WT and KO corneas in vivo. The results showed that an epithelial defect in central cornea was more rapidly resurfaced in the KO mouse compared with the WT mouse. The healing of the epithelial debridement was associated with the apoptosis of keratocytes and inflammatory cell invasion in the stroma beneath the defected epithelium.[39,40] Keratocytes in the peripheral cornea may migrate to the acellular stroma concomitant with epithelial repair.[39,40] The stroma of the intact cornea of the KO mouse was transparent and keratocytes were negative for αSMA. The transparency of the corneal tissue after the resurfacing of the debrided area was impaired in KO mice even though the epithelial healing was promoted by the gene ablation of Muc16 compared with WT mice. We hypothesized that IL-6 expressed in the conjunctiva of the KO mice might access the denuded stroma presumably via the tear fluid in the absence of an epithelial barrier and enhance both the macrophage invasion and the fibrogenic process by the newly invaded keratocytes during epithelial regeneration.[41,42] To answer this question, we examined the presence of keratocytes (ALDH3A1-positive) or myofibroblasts (αSMA-labeled) and macrophages in the stroma at 30 hours post debridement using immunohistochemistry. These results showed that more macrophages were observed in the KO cornea compared with the WT mice; that demonstrated our hypothesis. In the WT mice, the cells in the posterior stroma maintained the keratocyte phenotype and were labeled for ALDH3A1, while the fibroblastic cells in the anterior stroma were not labeled in the WT cornea. In the KO cornea, the majority of the cells in the stroma were negative for ALDH3A1. The fibroblastic cells in the KO stroma were αSMA-positive myofibroblasts while few myofibroblasts were seen in the WT cornea. Although immunohistochemistry obviously showed that a certain percentage of stromal cells lost the keratocyte phenotype and transformed into myofibroblasts more dramatically in the KO tissue compared with the WT stroma following the healing of the epithelial debridement, real-time PCR indicated no difference in the mRNA expression level of ALDH3A1 and αSMA. Explanations for this discrepancy might include that the alteration of the RNA expression pattern in the stroma of the central cornea beneath the regenerated epithelium might be masked by RNA in the peripheral intact cornea. (The RNA samples used were extracted from whole cornea with peripheral intact part.)

In conclusion, we have reported here that the loss of Muc16, a conjunctival mucin, affected the behaviors of the corneal epithelium and keratocytes. The mechanism might include the upregulation of inflammatory signaling cascade, such as Stat3 signal and the expression of IL-6 in the KO conjunctiva. The current data provided insights into the research of the pathophysiology of dry eye syndrome.

Acknowledgments

Previously presented by Shizuya Saika at the annual meeting of the Association for Research in Vision and Ophthalmology, Seattle, Washington, United States, May 2013.

Supported by United States Department of the Army Grant DAMD 17-03-1-0449, the Ben F. Love Endowment (RRB), a Bettyann Asche-Murray Ovarian Cancer Fellowship, and a Schissler Foundation Fellowship in Genetics of Human Disease (D-JC). The authors alone are responsible for the content and writing of the paper.

Disclosure: **K. Shirai**, None; **Y. Okada**, None; **D.-J. Cheon**, None; **M. Miyajima**, None; **R.R. Behringer**, None; **O. Yamanaka**, None; **S. Saika**, None

References

1. Mantelli F, Argueso P. Functions of ocular surface mucins in health and disease. *Curr Opin Allergy Clin Immunol*. 2008;8:477–483.
2. Gendler SJ, Spicer AP. Epithelial mucin genes. *Annu Rev Physiol*. 1995;57:607–634.
3. Vinall LE, Hill AS, Pigny P, et al. Variable number tandem repeat polymorphism of the mucin genes located in the complex on 11p15.5. *Hum Genet*. 1998;102:357–366.
4. Hanisch FG. O-glycosylation of the mucin type. *Biol Chem*. 2001;382:143–149.
5. Inatomi T, Spurr-Michaud S, Tisdale AS, Zhan Q, Feldman ST, Gipson IK. Expression of secretory mucin genes by human conjunctival epithelia. *Invest Ophthalmol Vis Sci*. 1996;37:1684–1692.
6. Rubin BK. Physiology of airway mucus clearance. *Respir Care*. 2002;47:761–768.
7. Murube J. The origin of tears. II. The mucinic component in the XIX and XX centuries. *Ocular Surf*. 2012;10:126–136.
8. Kyo Y, Kato K, Park YS, et al. Antiinflammatory role of MUC1 mucin during infection with nontypeable Haemophilus influenzae. *Am J Respir Cell Mol Biol*. 2012;46:149–156.
9. Kawashima H. Roles of the gel-forming MUC2 mucin and its O-glycosylation in the protection against colitis and colorectal cancer. *Biol Pharm Bull*. 2012;35:1637–1641.
10. Inatomi T, Spurr-Michaud S, Tisdale AS, Gipson IK. Human corneal and conjunctival epithelia express MUC1 mucin. *Invest Ophthalmol Vis Sci*. 1995;36:1818–1827.
11. Gipson IK. Distribution of mucins at the ocular surface. *Exp Eye Res*. 2004;78:379–388.
12. Pflugfelder SC, Liu Z, Monroy D, et al. Detection of sialomucin complex (MUC4) in human ocular surface epithelium and tear fluid. *Invest Ophthalmol Vis Sci*. 2000;41:1316–1326.
13. Argueso P, Spurr-Michaud S, Russo CL, Tisdale A, Gipson IK. MUC16 mucin is expressed by the human ocular surface epithelia and carries the H185 carbohydrate epitope. *Invest Ophthalmol Vis Sci*. 2003;44:2487–2495.
14. Wang Y, Cheon DJ, Lu Z, et al. MUC16 expression during embryogenesis, in adult tissues, and ovarian cancer in the mouse. *Differentiation*. 2008;76:1081–1092.
15. Danjo Y, Hazlett LD, Gipson IK. C57BL/6 mice lacking Muc1 show no ocular surface phenotype. *Invest Ophthalmol Vis Sci*. 2000;41:4080–4084.
16. Cheon D-J, Wang Y, Deng JM, et al. CA125/MUC16 is dispensable for mouse development and reproduction. *PLoS One*. 2009;4:e4675.
17. Saika S, Kawashima Y, Okada Y, et al. Immunohistochemical and ultrastructural analysis of dysplastic epithelium of human ocular surface: basement membrane and intermediate filament. *Cornea*. 1999;18:343–352.
18. Kokado M, Okada Y, Goto M, et al. Increased fragility, impaired differentiation, and acceleration of migration of corneal

epithelium of epiplakin-null mice. *Invest Ophthalmol Vis Sci*. 2013;54:3780–3789.

19. Okada Y, Reinach PS, Shirai K, et al. TRPV1 involvement in inflammatory tissue fibrosis in mice. *Am J Pathol*. 2011;178: 2654–2664.
20. Saika S, Okada Y, Miyamoto T, et al. Smad translocation and growth suppression in lens epithelial cells by endogenous TGFβ2 during wound repair. *Exp Eye Res*. 2001;72:679–686.
21. Saika S, Saika S, Liu CY, et al. TGFβ2 in corneal morphogenesis during mouse embryonic development. *Dev Biol*. 2001;240: 419–432.
22. Shirai K, Saika S, Tanaka T, et al. A new model of anterior subcapsular cataract: involvement of TGFβ/Smad signaling. *Mol Vis*. 2006;14:681–691.
23. Smart DE, Vincent KJ, Arthur MJ, et al. JunD regulates transcription of the tissue inhibitor of metalloproteinases-1 and interleukin-6 genes in activated hepatic stellate cells. *J Biol Chem*. 2001;276:24414–24421.
24. Sheng YH, Lourie R, Linden SK, et al. The MUC13 cell-surface mucin protects against intestinal inflammation by inhibiting epithelial cell apoptosis. *Gut*. 2011;60:1661–1670.
25. Guang W, Ding H, Czinn SJ, Kim KC, Blanchard TG, Lillehoj EP. Muc1 cell surface mucin attenuates epithelial inflammation in response to a common mucosal pathogen. *J Biol Chem*. 2010; 285:20547–20557.
26. Gubbels JA, Felder M, Horibata S, et al. MUC16 provides immune protection by inhibiting synapse formation between NK and ovarian tumor cells. *Mol Cancer*. 2010;9:11.
27. Blalock TD, Spurr-Michaud SJ, Tisdale AS, et al. Functions of MUC16 in corneal epithelia cells. *Invest Ophthalmol Vis Sci*. 2007;48:4509–4518.
28. Roy S, Sun Y, Pearlman E. Interferon-gamma-induced MD-2 protein expression and lipopolysaccharide (LPS) responsiveness in corneal epithelial cells is mediated by Janus tyrosine kinase-2 activation and direct binding of STAT1 protein to the MD-2 promoter. *J Biol Chem*. 2011;286:23753–23762.
29. Liang H, Baudouin C, Dupas B, Brignole-Baudouin F. Live conjunctiva-associated lymphoid tissue analysis in rabbit under inflammatory stimuli using in vivo confocal microscopy. *Invest Ophthalmol Vis Sci*. 2010;51:1008–1015.
30. Pflegerl P, Vesely P, Hantusch B, et al. Epidermal loss of JunB leads to a SLE phenotype due to hyper IL-6 signaling. *Proc Natl Acad Sci U S A*. 2009;106:20423–20428.
31. Zhang J, Yan X, Li H. Analysis of the correlations of Mucins, inflammatory markers, and clinical tests in dry eye. *Cornea*. 2013;32:928–932.
32. Mejias-Luque R, Peiro S, Vincent A, Van Seuningen I, de Bolos C. IL-6 induces MUC4 expression through gp130/ATAT3 pathway in gastric cancer cell lines. *Biochim Biophys Acta*. 2008;1783:1728–1736.
33. Yamada N, Yanai R, Inui M, Nishida T. Sensitizing effect of substance P on corneal epithelial migration induced by IGF-1, fibronectin, or interleukin-6. *Invest Ophthalmol Vis Sci*. 2005; 46:833–839.
34. Hernandez-Quintero M, Kuri-Harcuch W, Gonzalez Robles A, Castro-Munozledo F. Interleukin-6 promotes human epidermal keratinocyte proliferation and keratin cytoskeleton reorganization in culture. *Cell Tissue Res*. 2006;325:77–90.
35. Lennikov A, Kitaichi N, Fukase R, et al. Amelioration of ultraviolet-induced photokeratitis in mice treated with astaxanthin eye drops. *Mol Vis*. 2012;18:455–464.
36. Lin Z, Liu X, Zhou T, et al. A mouse dry eye model induced by topical administration of benzalkonium chloride. *Mol Vis*. 2011;17:257–264.
37. Xiao X, He H, Lin Z, et al. Therapeutic effects of epidermal growth factor on benzalkonium chloride-induced dry eye in a mouse model. *Invest Ophthalmol Vis Sci*. 2012;53:191–197.
38. Fredj-Reygrobellet D, Hristova D, Balas D, Senegas-Balas F. Immunohistological localization of regenerating protein in ocular structures. *Ophthalmic Res*. 1996;28:130–136.
39. Wilson SE. Corneal myofibroblast biology and pathobiology: generation, persistence, and transparency. *Exp Eye Res*. 2012; 99:78–88.
40. Wilson SE, Chaurasia SS, Medeiros FW. Apoptosis in the initiation, modulation and termination of the corneal wound healing response. *Exp Eye Res*. 2007;85:305–311.
41. Gallucci RM, Lee EG, Tomasek JJ. IL-6 modulates α-smooth muscle actin expression in dermal fibroblasts from IL-6-deficient mice. *J Invest Dermatol*. 2006;126:561–568.
42. Seong GJ, Hong S, Jung SA, et al. TGF-β-induced interleukin-6 participates in transdifferentiation of human Tenon's fibroblasts to myofibroblasts. *Mol Vision*. 2009;15:2123–2128.

Investigative Ophthalmology & Visual Science